

COMPUTER AIDED SEGMENTATION OF BRAIN TISSUES USING SOFT COMPUTING TECHNIQUES

¹Ramkumar, D., ²I. Jacob Raglend and ³K. Batri

¹Department of ECE, Theni Kammavar Sangam College of Technology, Theni, India

²Department of EEE, Noorul Islam Centre for Higher Education, Nagercoil, India

³Department of ECE, PSNA College of Engineering and Technology, Dindigul, India

Received 2014-01-30; Revised 2014-02-04; Accepted 2014-02-17

ABSTRACT

In this study, an efficient computer aided classification of brain tissue into Gray Matter (GM), White Matter (WM) and Cerebro-Spinal Fluid (CSF) is proposed. The proposed work consists of the following sub blocks like denoising, feature extraction and Classifier. This initial partition is performed by ANFIS after extracting the textural features like local binary pattern and histogram features. The main motivation behind this research work is to classify the brain tissue. By comparing the proposed method with other conventional methods, it is clear that our algorithm can estimate the correct tissues WM, GM and CSF much more accurately than the existing algorithms with respect to ground truth image patterns. We achieved an accuracy rate of 98.9% for Gray matter segmentation, 94.1% for White matter segmentation and 90.8% for CSF segmentation.

Keywords: Brain MRI, ANFIS, Curvelet, Medical Diagnostic Imaging, Medical Image Compression

1. INTRODUCTION

A medical image usually includes both useful and useless information in it. The useless information is referred to as noise and it can be eliminated without degrading the image. Many denoising algorithms are available which can reconstruct the original medical image by discarding the noise information. The analysis of the brain structure in normal case and in any disease case is a very challenging task in medical imaging. Structure of the brain is very complex; hence its study is also a very tough job. MRI is an excellent imaging method which provides a good contrast between the different tissues of the brain and gives accurate and rich information about the human brain anatomy compared to other medical imaging modalities.

In medical imaging, segmentation and feature extraction are the most important factors for diagnosis by an expert. MR image segmentation involves the separation of image pixels into regions comprising different tissue types. All MR images are affected by

random noise. The noise comes from the stray current in the detector coil due to the fluctuating magnetic fields arising from random ionic currents in the body, or the thermal fluctuations in the detector coil itself. When the level of noise is significant in an MR image, tissues that are similar in contrast could not be delineated effectively, causing error in tissue segmentation.

In this study, we have proposed an automatic intelligent system for the classification of brain structure into three regions: GM, WM and CSF based on the textural features. We use curvelet transform for noise removal while the texture based classifier is built using Adaptive Neuro Fuzzy Interference System (ANFIS), one of the most widely used supervised learning algorithms in many medical imaging applications. The main contributions of the proposed technique include as follows: This technique efficiently removes noise from the brain MR image without degrading the quality of the image and accurately segments the brain MR image into three tissue classes based on the textural features.

Corresponding Author: Ramkumar, D., Department of ECE, Theni Kammavar Sangam College of Technology, Theni, India

1.1. Related Works

Zanaty (2012) proposed a hybrid approach based on combining fuzzy clustering, seed region growing and Jaccard similarity coefficient algorithms to Measure Gray (GM) and White Matter tissue (WM) volumes from Magnetic Resonance Images (MRIs). This algorithm incorporates intensity and anatomic information for segmenting of MRIs into different tissue classes-GM and WM. First, it partitions the image into different regions using fuzzy clustering. These regions are fed to Seed Region Growing (SRG) method to isolate the suitable closed region. The seeds of SRG are selected as the output centers of the fuzzy clustering method. Jaccard similarity coefficient is used to merge the similar regions in one segment. The experimental results showed that the technique produces accurate and stable results.

Sepehrband *et al.* (2010) has presented an efficient medical image transformation method for lossless compression by considering real time applications.

Can *et al.* (2013) presented a Voxel-Based Morphometry (VBM) study to identify gray matter and white matter concentrations in infants. Early gray matter concentration in the right cerebellum, early white matter concentration in the right cerebellum and early white matter concentration in the left Posterior Limb of the Internal Capsule (PLIC)/cerebral peduncle were strongly associated with the receptive language ability of the infant at 12 months. Early gray matter concentration in the right hippocampus was positively and strongly correlated with the expressive language ability of the infant at 12 months. Their results showed that the cerebellum, PLIC/cerebral peduncle and the hippocampus were associated with early

language development. Also they discussed that these structural predictors are closely related to the linguistic functions of the infants.

Feng *et al.* (2011) presented an R package for Magnetic Resonance Imaging (MRI) tissue classification. The methods include using normal mixture models, hidden Markov normal mixture models and a higher resolution hidden Markov normal mixture model by various optimization algorithms and by a bayesian Markov Chain Monte Carlo (MCMC) method.

Harati *et al.* (2011) proposed a computer-assisted classification method which combines conventional MRI and perfusion MRI for differential diagnosis. Their method consists of several steps including ROI definition, feature extraction, feature selection and classification. The extracted features include tumor shape and intensity characteristics as well as rotation invariant texture features. Features subset selection is performed using Support Vector Machines (SVMs) with recursive feature elimination.

Vishnuvarthanan and Rajasekaran (2013) used fuzzy algorithm for the detection and segmentation of brain tumors in MRI brain image. The average tumor segmentation time is 30 sec, which leads to high computational time.

1.2. Proposed Pattern

Among the brain MRI regions, the white matter and gray matter are the most important, since most of the tumors occur in these regions. We propose an ANFIS based classification system for the separation of white matter, gray matter and Cerebro-Spinal Fluid (CSF) regions. The overall block diagram of the proposed automated system is illustrated in Fig. 1.

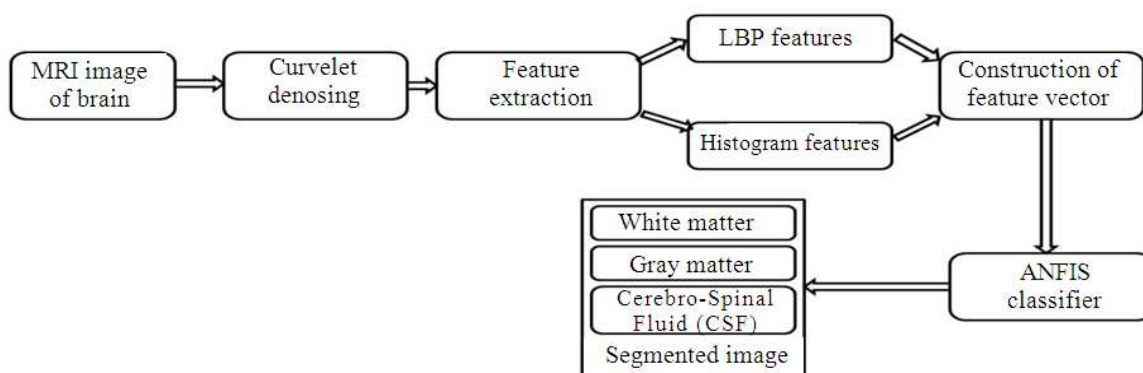


Fig. 1. Proposed flow of our classification system

2. MATERIALS AND METHODS

2.1. Collection of Real Data Sets

Several 2-D MRI data sets are collected from the web source: www.brainweb.org. The data sets belong to adults aged between 18 and 60 years. Totally, 90 MRI brain images were utilized as test images. The features of all the images collected for our experiment are:

- T1-weighted brain MRI (30 images)
- T2-weighted brain MRI (30 images)
- Fluid Attenuated Inversion Recovery (FLAIR) MRI (30 images)

2.2. Noise Reduction Using Curvelet Transform

The noises in the brain MRI image are eliminated by using curvelet transforms which represents the edges and curves very effectively only by using fewer coefficients compared to other standard transforms. Noises like Random noise, Gaussian noise, Poisson noise are added to the image and denoised using the curvelet transform algorithm. The performance of curvelet transform is evaluated and the results are obtained by Equation 1:

$$X_{i,j} = f(i,j) + \sigma_z(i,j) \quad (1)$$

Where:

f = The image to be recovered and

z = The white Gaussian noise

2.2.1. The Denoising Algorithm

The implementation of curvelet transform consists of the following steps:

- Step1: Compute all the threshold values for curvelet.
- Step2: Compute the norm of curvelet.
- Step3: Apply curvelet transform to the noisy image.
- Step4: Apply hard thresholding to the curvelet coefficients.
- Step5: Apply inverse curvelet transform to the result of step 4.

2.3. Local Binary Pattern (LBP) Features

Local Binary Pattern (LBP) is an efficient texture based operator. It works by labelling the pixels of an image by thresholding the neighbourhood of each pixel and stores the result as a binary number. The LBP

operator is more robust to monotonic gray-scale changes caused by illumination variations. Also, this LBP operator has a computational simplicity; hence it is possible to analyze the images in real-time applications.

2.2.1. LBP Operation over Spatial Domain

The LBP operator defines a two-Dimensional surface texture by 2 complementary measures, namely, gray scale contrast and local spatial patterns. The original LBP operator creates labels for the pixels in the image by thresholding the 3x3 surrounding pixels with the centre value and stores the result as a binary number. Thus, the histogram values for these $2^8 = 256$ different labels are used as texture descriptors. In unsupervised pattern segmentation, LBP operator can be used in combination with a local contrast measure to produce higher performance.

The LBP operator was further developed to utilize the different sized neighbourhoods. A varying radius and number of pixels in the neighbourhood is allowed by using a circular neighbourhood and bilinear interpolating values. The variance in gray-scale of the local neighbourhood can be employed as the corresponding contrast measure. The pixel neighbourhoods are given by, (P, R), where P is the set of sampling points over a circle of radius of R as shown in **Fig. 2**. LBP is said to be uniform if the binary pattern consists of almost 2 bit-wise transitions from 0 to 1 or 1 to 0, when the bit pattern traverses circularly. Consider, the patterns 00000000 (0 transitions), 11001111 (2 transitions) and 01110000 (2 transitions) are uniform, whereas the patterns 11001001 (4 transitions) and 01010010 (6 transitions) are not uniform. During the LBP computation of labels, only uniform patterns are considered so that each uniform pattern has an individual label and all the non-uniform patterns are labelled with another single individual label. Consider the example, when using (8, R) neighbourhood, there exists 256 patterns out of which 58 are uniform yielding 59 different labels.

The LBP operator is defined by, $LBP_{(P,R)}^{u2}$ where, (P,R) represents the LBP operator used in a (P,R) neighbourhood, 'u2' defined that only uniform patterns are used and labelling all other patterns with a single label. On obtaining the LBP labelled image $f_i(x, y)$, the LBP histogram H_i can be defined as Equation 2:

$$H_i = \sum_{x,y} I\{f_i(x, y) = i\} \quad i = 0, 1, \dots, n-1 \quad (2)$$

where, 'n' is the number of LBP labels and $I\{A\}$ is 1 if A is true and 0 if A is false.

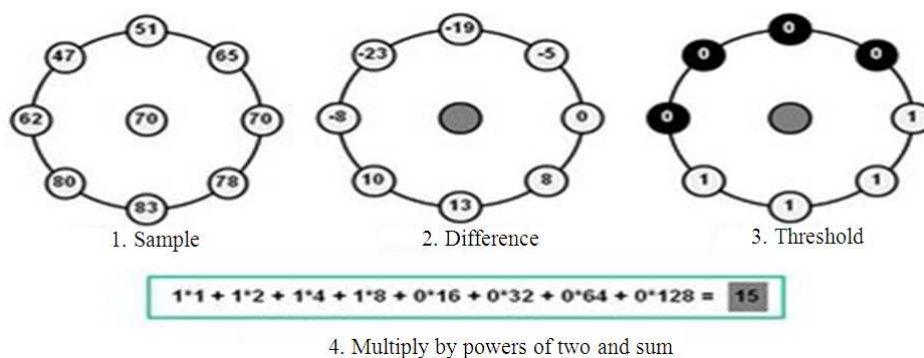


Fig. 2. LBP computation

If the histograms are of different sizes, then it must be normalized to get a consistent description in contrast by using Equation 3:

$$N_i = H_i \sum_{j=0}^{n-1} H_j \quad (3)$$

2.4. Histogram Features

2.4.1. Histogram-Definition

A histogram is a graphical plot which represents the frequency of occurrence of image pixels. Though, it resembles a bar-chart it should never be confused with it. Histograms were built on the idea of dot-plots but its use is limited to samples of continuous variables. An interval on the number line which completely encompasses the data, from the sample minimum to its maximum, is subdivided into smaller intervals called ‘bins’.

The bins usually have the same width and bin-width. The frequency of sample values inside each bin is calculated and a rectangle is constructed, based on each bin. The height of the rectangle represents the frequency of occurrence and it equals to frequency in the corresponding bin divided by its bin-width. Thus, the area of the rectangle represents the count of sample values in the bin. Suppose if all the bins have the same width, then the area of each rectangle will be in the same fraction to its height. All the samples should be represented in only one bin in the histogram in case of equal bin widths.

A model histogram with sample values: 4.3, 4.4, 5.2, 5.6, 6.0, 6.4, 6.8, 7.1, 7.4, 7.4, 8.2, 8.2, 8.7, 9.2, 9.6, 10.0, 10.0, 10.5, 11.8 is shown in **Fig. 3**.

The histogram resembles a dot-plot if the bin widths are narrower and if it is broad, the sample becomes void. The optimal choice for bin width depends on the sample size and the range of data.

2.4.2. Gray-Scale Histogram

The gray-scale histogram of an image represents the distribution of the pixels over the gray-level scale. It can be visualised as if each pixel is placed in a bin corresponding to the colour intensity of that pixel. The entire pixels in each bin are summed up and plotted on a graph, which gives the image histogram. **Figure 4** illustrates the histogram of a sample image. The image is analysed based on the frequencies of all the intensity levels.

2.4.3. Histogram Equalization

The histogram of an image is equalized for contrast adjustment. By means of histogram equalization, the intensities get distributed better over the histogram. This allows areas of lower contrast to get better contrast. This method achieves this by efficiently spreading out the most frequently occurring intensity values. This method is useful for images with both backgrounds and foregrounds dark or both bright. In our paper, this method helps to get a better view of GM, WM and CSF in brain MR images even if the MRI is bright or dark. Histogram equalization makes contrast adjustment in brain MR image such that the soft tissues in the image become clearly detectable.

2.5. Adaptive Neuro Fuzzy Interference systems

Adaptive Neuro Fuzzy Interference Systems (ANFIS) are adaptive networks implemented in MATLAB software. An adaptive network consists of a group of nodes and directional links. The network has a learning rule such as back propagation. ANFIS is said to be adaptive because some or all the nodes have parameters which influences the output node. ANFIS is a supervised learning technique and relates the inputs with the outputs.

The ANFIS architecture is shown in **Fig. 5**. The circular nodes in the figure are fixed nodes and the square nodes have parameters to be trained.

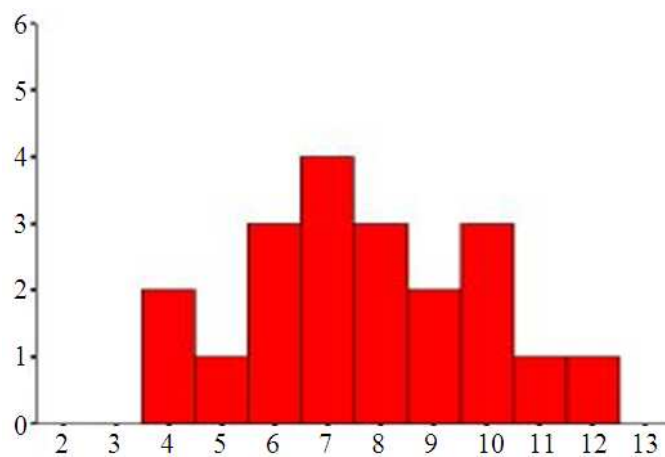


Fig. 3. A sample Histogram with 9 bins

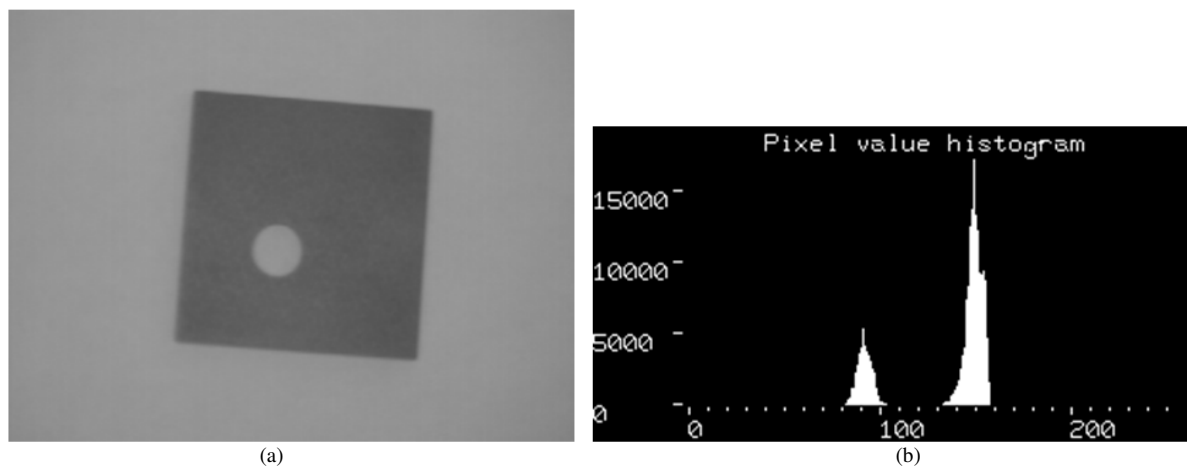


Fig. 4. (a) Example of an image and (b) its histogram

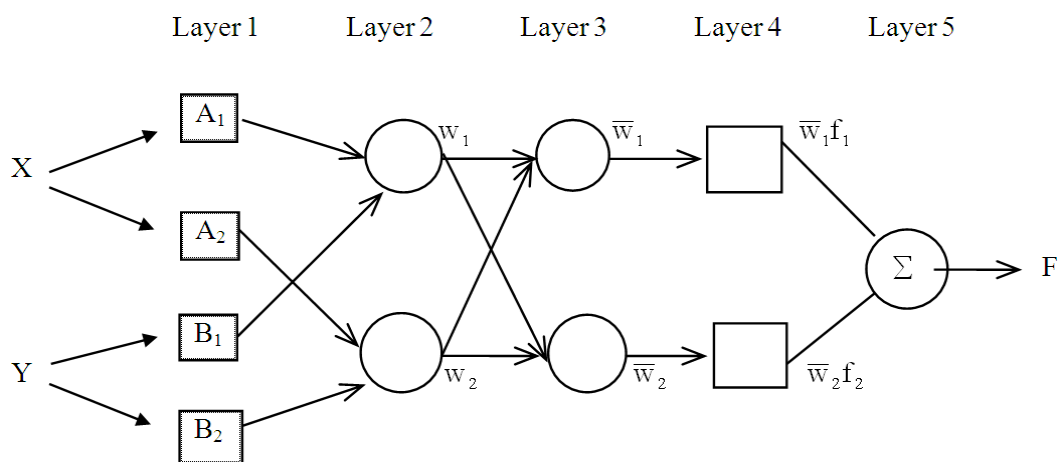


Fig. 5. ANFIS architecture for a two rule system

Consider an ANFIS classifier based on a Two-rule system as below:

If x is A1 and y is B1 then, $f_1 = p_1x + q_1y + r_1$
 If x is A2 and y is B2 then, $f_2 = p_2x + q_2y + r_2$

For the training of the network, there is a forward pass and a backward pass. We now look at each layer in turn for the forward pass. The forward pass propagates the input vector through the network layer by layer. In the backward pass, the error is sent back through the network in a similar manner to back propagation.

2.5.1. Layers of ANFIS Architecture

Layer 1

At layer1, the output of each node is given by:

$$O_{1,i} = \mu_{A_i}(x) \text{ for } i = 1,2$$

$$O_{1,i} = \mu_{B_{i-2}}(y) \text{ for } i = 3,4$$

where, $O_{1,i}(x)$ is essentially the member for x and y . The membership function we have considered is a bell shaped function given by Equation 4:

$$\mu_A(x) = \frac{1}{1 + \left| \frac{x - c_i}{a_i} \right|^{2b_i}} \tag{4}$$

where a_i, b_i, c_i are the ground parameters to be trained.

Layer 2

In this layer, all the nodes are fixed. Here, the t-norm is used to ‘AND’ the membership grades, for example, the product given by Equation 5:

$$O_{2,i} = w_i = \mu_{A_i}(x)\mu_{B_i}(y), i = 1,2 \tag{5}$$

Layer 3

Layer 3 contains fixed nodes which calculate the ratio of the firing strengths of the rules, as given below Equation 6:

$$O_{3,i} = \bar{w}_i = \frac{w_i}{w_1 + w_2} \tag{6}$$

Layer 4

In this layer, the nodes are adaptive and achieve the consequent of the rules Equation 7:

$$O_{4,i} = \bar{w}_i f_i = \bar{w}_i (p_i x + q_i y + r_i) \tag{7}$$

The parameters in this layer (p_i, q_i, r_i) are to be determined and are referred to as the consequent parameters.

Layer 5

In this layer, a single node is present which computes the overall output Equation 8:

$$O_{5,i} = \sum_i \bar{w}_i f_i = \frac{\sum_i w_i f_i}{\sum_i w_i} \tag{8}$$

Then, the input vector is fed through the network layer by layer. We now consider how the ANFIS learns the premise and consequent parameters for the membership functions and the rules.

2.5.2. Operation of ANFIS Classification

For an ANFIS adaptive network with fixed premise parameters, the output is linear in the consequent parameters. The total parameter can be categorized into three:

- S = set of total parameters
- S_1 = set of premise parameters
- S_2 = set of consequent parameters

ANFIS employs a 2-pass supervised learning algorithm, which consists of, a Forward Pass and a Backward Pass. The steepest descent algorithm is used along with the least squares algorithm to adapt to the parameters in this ANFIS algorithm.

2.5.3. The Forward Pass

Here S_1 is fixed and S_2 is estimated using a Least Squares algorithm. The procedure is as follows:

- Step1: Feed the input vector
- Step2: Compute the output at each node and at each layer
- Step3: Repeat for all data $\rightarrow A$ until y is produced
- Step4: Find the parameters in S_2 using Least Squares
- Step5: Calculate the error for each training pair

2.5.4. The Backward Pass

Here S_2 is fixed and S_1 is estimated using back propagation. The parameters in S_1 are updated by back

propagation for given fixed values of S_1 and these parameters are assured to be the global optimal point.

3. RESULTS

Numerous simulations were performed and the results are given as follows. The original image used for our experimentation is shown in **Fig. 6**. The ground truth images as predicted by a physician and the final segmented images using our proposed method are illustrated in **Fig. 7**.

The performance comparisons of various parameters of proposed and existing methods are done and their values are plotted graphically in **Fig. 8**.

Table 1-3 illustrates the performance evaluation of the segmented images into Gray Matter (GM), White Matter (WM) and Cerebro-Spinal Fluid (CSF) regions, respectively. The performance of brain tissue segmentation is analyzed with the following parameters:

- Sensitivity [$Se = TP/(TP+FN)$]
- Specificity [$Sp = TN/(TN+FP)$]
- Positive predictive value [$Ppv = TP/(TP+FP)$]
- Negative predictive value [$Npv = TN/(TN+FN)$]
- Accuracy [$Acc = (TP+TN)/(TP+FN+TN+FP)$]

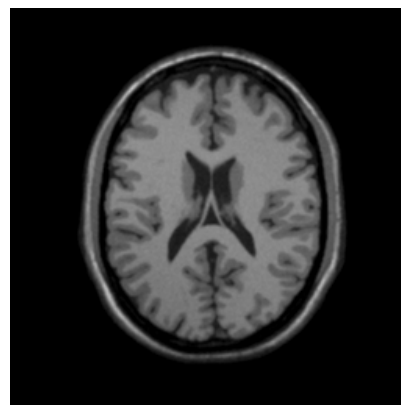


Fig. 6. Source brain MR image

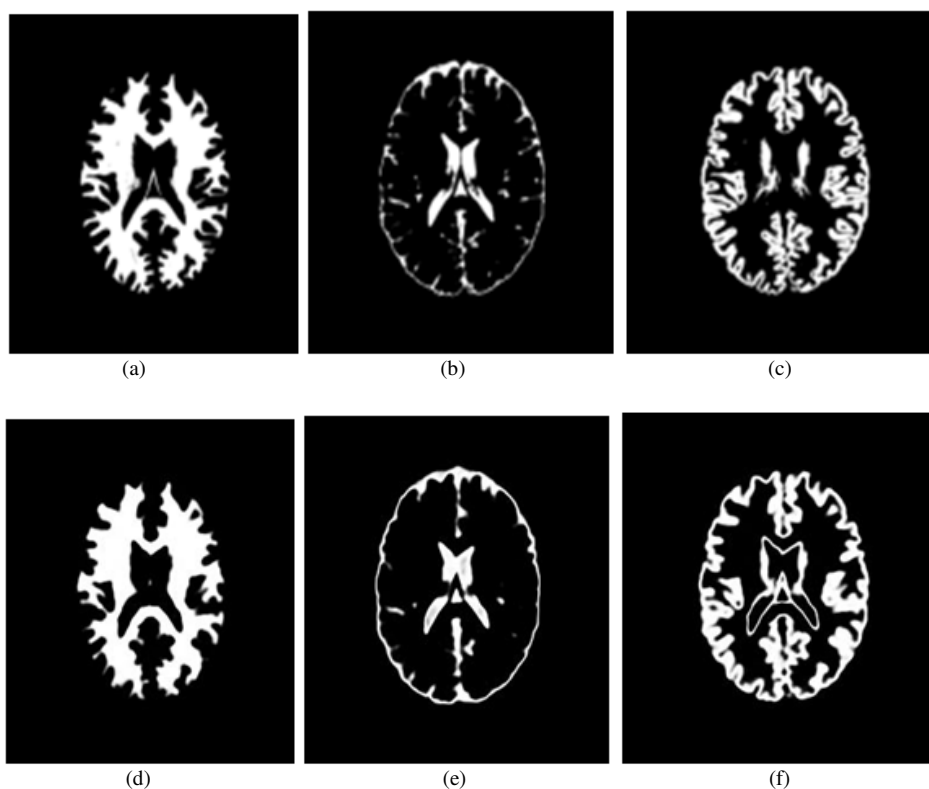


Fig. 7. Comparison of segmented images with ground truth images: (a)-(c) Ground truth images showing White matter, Gray matter and CSF respectively, (d)-(f) Segmented images obtained by proposed technique showing White matter, Gray matter and CSF respecti

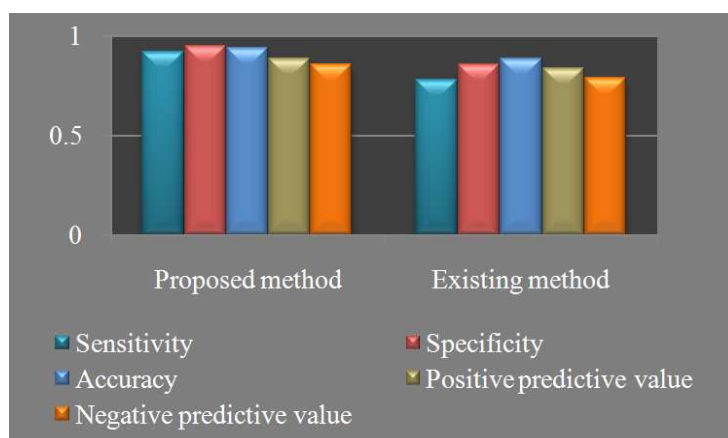


Fig. 8. Graphical representations of performance comparison of proposed method with existing method

Table 1. Performance evaluation of Gray matter segmentation

| Images | Se | Sp | Ppv | Npv | Acc |
|---------|----------|----------|----------|----------|----------|
| 1 | 0.597300 | 1.091600 | 0.718800 | 1.043700 | 0.986100 |
| 2 | 0.599900 | 1.091900 | 0.720100 | 1.044800 | 0.987200 |
| 3 | 0.619500 | 1.102800 | 0.772900 | 1.043900 | 0.995900 |
| Average | 0.605540 | 1.095413 | 0.737275 | 1.044116 | 0.989716 |

Se = Sensitivity; Sp = Specificity; Acc = Accuracy; Ppv = Positive Predictive Value; Npv = Negative Predictive Value

Table 2. Performance evaluation of White matter segmentation

| Images | Se | Sp | Ppv | Npv | Acc |
|---------|----------|----------|----------|----------|----------|
| 1 | 0.990500 | 1.166300 | 1.066300 | 1.144300 | 0.940700 |
| 2 | 0.988800 | 1.165200 | 1.061600 | 1.143900 | 0.939700 |
| 3 | 0.985600 | 1.174500 | 1.100000 | 1.140900 | 0.944000 |
| Average | 0.988305 | 1.168670 | 1.075966 | 1.143014 | 0.941437 |

Se = Sensitivity; Sp = Specificity; Acc = Accuracy; PPV = Positive Predictive Value; NPV = Negative Predictive Value

Table 3. Performance evaluation of CSF segmentation

| Images | Se | Sp | Ppv | Npv | Acc |
|---------|----------|----------|----------|----------|----------|
| 1 | 0.218000 | 1.099000 | 0.443200 | 0.965900 | 0.911000 |
| 2 | 0.216000 | 1.098400 | 0.437900 | 0.966000 | 0.910600 |
| 3 | 0.215900 | 1.099600 | 0.455000 | 0.956800 | 0.904100 |
| Average | 0.216601 | 1.099008 | 0.445362 | 0.962897 | 0.908582 |

Se = Sensitivity; Sp = Specificity; Acc = Accuracy; PPV = Positive Predictive Value; NPV = Negative Predictive Value

These parameters are evaluated and listed in **Table 1-3**, where, TP denotes true positive, FP denotes false positive, FN is false negative and TN is true negative. True Positive refers to the correctly identified GM/WM/CSF pixels, True Negative refers to the wrongly identified GM/WM/CSF pixels, False Positive refers to the correctly identified non-GM/WM/CSF pixels and False Negative refers to the wrongly identified non-GM/WM/CSF pixels.

The entire algorithm was run on MATLAB and the segmentation results were obtained. The MATLAB R2008

is used to simulate and evaluate the proposed method. It takes 11 sec per image on an average to run on a 2.8 GHz Intel Pentium Core i3 machine with 4GB of internal RAM.

4. DISCUSSION

The proposed segmentation algorithm has been designed using MATLAB software. The data set used in our method has been taken from www.brainweb.org. A collection of normal and abnormal brain images were made use of from the web source.

Table 4. Performance Comparison of proposed classification with other methods

| | Se | Sp | Acc | Ppv | Npv |
|-----------------|------|------|------|------|------|
| Proposed method | 0.92 | 0.95 | 0.94 | 0.89 | 0.86 |
| Existing method | 0.78 | 0.86 | 0.89 | 0.84 | 0.79 |

Se = Sensitivity; Sp = Specificity; Acc = Accuracy; Ppv = Positive Predictive Value; Npv = Negative Predictive Value

The segmentation algorithm was implemented over a MRI brain image (**Fig. 6**) and the results of segmentation were compared with their respective ground truth images. The proposed technique showed an accuracy of 94%.

The parameters considered for evaluating the algorithm are Sensitivity, Specificity, Positive predictive value, Negative predictive value and Accuracy. Sensitivity and Specificity define the ratio of well-classified GM/WM/CSF and non-GM/WM/CSF pixels, respectively. Positive predictive value is the ratio of pixels classified as tissue pixels that are correctly classified. Negative predictive value is the ratio of pixels classified as background pixels that are correctly classified. Lastly, Acc is the ratio of total well-detected and classified GM/WM/CSF pixels. All these parameters help in defining the performance of our proposed classification technique.

The various performance parameters of our proposed algorithm are compared to the existing methodology and are tabulated in **Table 4**. The comparison results prove that our proposed method stands high in terms of accuracy of segmentation.

5. CONCLUSION

In this study, the computer aided segmentation of brain tissues into Gray Matter (GM), White Matter (WM) and Cerebro-Spinal Fluid (CSF) is proposed. The proposed work consists of sub-blocks like denoising, feature extraction and Classifier.

On comparing the performance of the proposed method with that of other conventional methods, it is clear that our algorithm estimates the correct tissues WM, GM and CSF much more accurately than the established algorithms. The main limitation of this study is that it has low positive predictive and accuracy value. Future research in MRI segmentation should attempt towards the improvement of the computational speed of the segmentation algorithms.

6. REFERENCES

- Can, D.D., T. Richards and P.K. Kuhl, 2013. Early gray-matter and white-matter concentration in infancy predict later language skills: A whole brain voxel-based morphometry study. *Brain Lang.*, 124: 34-44. DOI: 10.1016/j.bandl.2012.10.007
- Feng, D. and L. Tierney, 2011. Mritc: A package for MRI tissue classification. *J. Stat. Software*, 44: 1-20.
- Vishnuvarthanan, G. and M.P. Rajasekaran, 2013. Segmentation of MR Brain images for tumor extraction using fuzzy. *Current Med. Imag. Rev.*, 9: 2-6.
- Harati V., R. Khayati and A. Farzan, 2011. Fully automated tumor segmentation based on improved fuzzy connectedness algorithm in brain MR images. *Comput. Biol. Med.*, 41: 483-492. DOI: 10.1109/42.511758
- Sepehrband, F., M. Mortazavi, S. Ghorshi and J. Choupan, 2010. Efficient medical image transformation method for lossless compression by considering real time applications. *Proceedings of 4th International Conference on Signal Processing and Communication Systems*, Dec. 13-15, IEEE Xplore Press, Gold Coast, QLD, pp: 1-8. DOI: 10.1109/ICSPCS.2010.5709763
- Zanaty, E.A., 2012. Determination of Gray Matter (GM) and White Matter (WM) volume in brain Magnetic Resonance Images (MRI). *Int. J. Comput. Applic.*, 45: 16-22. DOI: 10.1109/TIP.2005.871116